

NAGI-685

LANGLEY
GRANT

IN-39

9/29/5

CR

p. 29



FLORIDA ATLANTIC UNIVERSITY

College of Engineering • Department of Ocean Engineering

Center for Acoustics and Vibrations



(NASA-CR-180282) EXTENSION OF VIBRATIONAL
POWER FLOW TECHNIQUES TO TWO-DIMENSIONAL
STRUCTURES Annual Report No. 1 (Florida
Atlantic Univ.) 29 p Avail: NTIS HC
A03/MF A01

N87-27265

Unclas

CSCD 20K G3/39 0091295

EXTENSION OF VIBRATIONAL
POWER FLOW TECHNIQUES TO
TWO-DIMENSIONAL STRUCTURES

J. M. Cuschieri
Center for Acoustics and Vibration
Department of Ocean Engineering
Florida Atlantic University
Boca Raton, Florida 33431

August 1987

First Annual Report
Grant Number NAG - 1 - 685

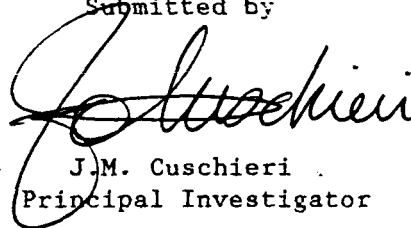
Submitted to

National Aeronautics and Space Administration
Langley Research Center
Hampton VA 23665

FORWARD

This report describes the work done in the second half of the first year under Research Contract Number NAG - 1 - 685, entitled "Use of Energy Accountancy and Power Flow Techniques for Aircraft Noise Transmission". The financial support by Nasa Langley to pursue this research work is greatly appreciated. The author would also like to acknowledge the assistance of Ms McCollum, Mr. J.L. Rassineux, and Mr. T. Gibert and for their contributions and work in this research effort.

Submitted by

A handwritten signature in dark ink, appearing to read "J.M. Cuschieri", is written over the printed name and title.

J.M. Cuschieri
Principal Investigator

Abstract

In the analysis of the vibration response and structure-borne vibration transmission between elements of a complex structure, statistical energy analysis (SEA) or finite element analysis (FEA) are generally used. However, an alternative method is using vibrational power flow techniques which can be especially useful in the mid frequencies between the optimum frequency regimes for FEA and SEA. Power flow analysis has in general been used on one-dimensional beam-like structures or between structures with point joints. In this paper, the power flow technique is extended to two-dimensional plate like structures joined along a common edge without frequency or spatial averaging the results, such that the resonant response of the structure is determined. The power flow results are compared to results obtained using FEA at low frequencies and SEA at high frequencies. The agreement with FEA results is good but the power flow technique has an improved computational efficiency. Compared to the SEA results the power flow results show a closer representation of the actual response of the structure.

Introduction

The use of power flow techniques for the analysis of the vibration response and structure-borne vibration transmission between elements of a structure has in general been restricted to either one-dimensional beam type structures [1,2] or to structural elements with only point attachments [3]. The problem of line joints between structural elements has only been studied using power flow techniques averaged over defined frequency bands (one-third octave frequency bands) [4] in which case the results that are obtained are identical to those of statistical energy analysis (SEA). Thus, the potential of the structural power flow method to give results for the detailed structural response for the elements of the structure, which as shown in [1] can be very important in the mid frequency range is completely lost.

The basic concepts of the power flow method and its application to determine the transmitted power have been demonstrated in a number of published papers [1,2]. In the previous paper by this author comparisons were also made between the results obtained using the power flow technique and results obtained using both SEA and finite element analysis (FEA). As shown in that paper [1] while FEA and SEA are excellent tools to be used in the low and high frequency regimes, respectively, a gap is left in the mid-frequency range where FEA becomes computationally unwieldy, and SEA would only give mean response levels with the actual response of the structure, especially near resonances, being potentially significantly different from these mean levels. The gap in the mid-frequency range, between FEA and SEA, can be satisfied using the power flow techniques. In fact since FEA and SEA are well established tools, these can be used to determine the results at low and high frequencies. These results are then compared to results obtained using the power flow method in these frequency regimes and by ensuring that there is a good match between the two sets of results in each respective frequency range, this can serve as a verification of the power flow model.

Following is a brief general outline of the power flow method. The structure is modeled by a series of coupled substructures with forces or moments introduced at the joints between the substructures. The power flow into the source substructure and between the substructures is expressed in terms of input (point, line or area) and transfer structural mobility functions. The definition of structural mobility is the ratio of rate of change of displacement (translational or rotational) per unit input load. For point mobilities the response and the load are measured at the same location, while for transfer mobilities the response and the load are at separate locations. The exact definition of the mobility functions to be used at the different joints between the substructures will depend on the type and configuration of the joint. The detailed response for the structural response of the elements of the structure is obtained by ensuring that the mobility function used in the analysis are not spatially or frequency averaged.

The use of the power flow analysis for the determination of the response of a two-dimensional plate-like structure is presented in this paper. In the analysis two plates are joined at right angles along a common edge and one of the plates, the source plate substructure is excited by a point force. The transmitted vibrational power, to the attached second plate, the receiver plate, presented both per unit input force and as a ratio to the input power, is computed. The results obtained using the power flow technique are then compared to results obtained using FEA and SEA. However, in this case, unlike what was done in [1] the comparisons are restricted to low and high frequency regimes respectively. With FEA the computation time required to obtain the transmitted power as a function of frequency were becoming prohibitively long as the frequency range increased.

L-Shaped Plate Structure

Using the power flow method, the vibrational power transmitted between two plates joined along a common edge to form an L-shaped plate is computed. One of the plates is excited by a point load arbitrarily located, but initially the excitation location is kept away from the common edge. The L-shaped plate, coordinate system and loading are shown in figure (1). The following conditions were assumed for the two plates.

1. The plates are thin compared to the wavelength so that inplane forces, rotary inertia and shear can be neglected.
2. The joint between the two plates is a pinned joint.

These conditions were only assumed such that some boundary conditions can be defined. However, other boundary conditions and the analysis for thick plates, where inplane forces and rotary inertia and shear are important can be analyzed in a similar fashion. In fact, thick plates with different boundary conditions are presently being investigated.

Using the power flow method, a model for the structure is first defined. In general, a power flow model consist of a number of source and receiver substructures for which ways of obtaining the mobility functions are available. For the L-shaped plate structure considered here, the structure is divided into two substructures which are joined at the edge. For the L-shaped plate structure considered here, the structure is divided into two substructures which are joined at the edge. In general terms, using the two substructure model with one force input, shown in figure (2) the expressions for the input and transmitted power are [2]

$$\frac{P_{in}}{|F(f)|^2} = \frac{1}{2} \text{ Real } \left\{ M_1 - \frac{M_{12} M_{21}}{M_2 + M_3} \right\} \quad (1)$$

$$\frac{P_{\text{trans}}}{|F(f)|^2} = \frac{1}{2} \left| \frac{M_{12}}{M_2 + M_3} \right|^2 \text{Real} \left\{ M_3 \right\}$$

(2)

where M_i , $i = 1, 2, 3$ are the input mobilities at locations 1, 2 and 3 and M_{12} and M_{21} are the transfer mobilities.

In the case of the L-plate structure with point load excitation, M_1 would be the input mobility for the source plate substructure when isolated from the receiver substructure. The input mobility here would be the normal surface velocity at the excitation location per unit applied load. M_2 and M_3 represent input mobilities for the source and receiver plate substructures respectively, at the location of the joint between the substructures. However, because the plates are joined along an edge, the definition of these mobility functions is different from that of M_1 . M_2 and M_3 will represent the rate of change of displacement, translational and rotational at all the points along the junction edge of the plate, per unit applied inplane, transverse and moment loads. The motion at every location along the junction will be dependent not only on the loading at that location but on the load distribution along the entire edge. To ensure that the results to be obtained from the analysis are relevant to the solution to the response of the global structure, the distribution of the loading along the edge must be identified. M_{12} and M_{21} represent the transfer mobilities between the excitation location and the joint location respectively and vice versa. In this case as well, similar to M_2 and M_3 , because the joint is along one edge the transfer mobilities will be defined as follows. M_{12} is given by the ratio of the rate of change of displacement (also translational and rotational) at every location along the joint and the applied loading. Thus M_{12} will in general be a function of the location along the edge. M_{21} is given by the ratio of the rate of change of displacement at the location where the excitation is applied per unit applied loading along the edge.

Since some of the mobility functions described in the previous paragraphs are function of the location along the edge, the power transmitted will thus be given by an integral over the entire length of the joint.

Thus far, the discussion on the required mobilities, has been restricted to general definitions in the context of two-dimensional structures joined along a common edge. Since the assumptions are being made that the plates are thin compared to the wavelength and that no transverse motion is allowed at the joint, some simplifications can be made to the definition of the mobility functions. For thin plates the main type of motion under transverse loading is bending or the generation of flexural waves. If only transverse displacements are considered, the excitation along the joint edge will be in the form of a distributed moment. Thus the parameters that one is dealing with for the particular case studied here

are, a point load, transverse displacement at the point of application of this load, a distributed moment along one edge and rotational displacement along this same plate edge.

Having developed the power flow model for the problem and identified the required mobility functions and their respective definitions, the next step is to develop expressions for these mobility function. In developing these mobility expressions, it is not necessary to consider the global structure but each substructure is considered separately. For the L-plate problem, each substructure consists of a flat plate structure and thus in developing the mobility functions a flat plate with the different types of loading as described above needs to be considered. Thus the analysis of the L-plate structure is simplified to the analysis of flat plate structures.

In deriving an expression for M_1 , a plate with the loading as shown in figure (3(a)) is considered. The boundary conditions of the plate are the same as those for the global structure, that is all edges are pinned or simply supported and therefore the boundary condition are zero displacement and zero bending moment. Since a thin plate is being considered, the response can be expressed in terms of a series solution with assumed mode functions that satisfy the defined boundary conditions. Thus for M_1 [5]

$$\begin{aligned}
 M_1(f) &= \frac{V(x_o, y_o, f)}{F(f)} \\
 &= \frac{j2f}{\pi \rho h a b} \sum_{n=1}^{\infty} \frac{\sin^2\left(\frac{n_1 \pi x_o}{a}\right) \sin^2\left(\frac{n_2 \pi y_o}{b}\right)}{\left[(f_n^*)^2 - f^2\right]}
 \end{aligned} \tag{3}$$

where f is the frequency, a and b are the width and length of the plate, ρ is the plate material density and h is the plate thickness. f_n is the n th damped natural frequency of the plate given by

$$f_n^* = \sqrt{\left(\frac{D}{\rho h}\right) \left[\left(\frac{n_1 \pi}{a}\right)^2 + \left(\frac{n_2 \pi}{b}\right)^2 \right]} \tag{4}$$

where D^* is the plate complex flexural rigidity which includes structural damping and n represents the double subscript (n_1, n_2) .

An expression for M_{12} can also be derived from this plate configuration since M_{12} represents the angular displacement along one edge of the plate, which would be the joint edge per unit applied force when a transverse load is applied somewhere on the plate. That is

$$M_{12}(x) = \frac{\dot{\theta}(x, b, f)}{F(f)} = \frac{j2f}{\rho h a b^2} \cdot \sum_{n=1}^{\infty} \frac{(-1)^{n_2} n_2 \sin\left(\frac{n_1 \pi x}{a}\right) \sin\left(\frac{n_1 \pi x_0}{a}\right) \sin\left(\frac{n_2 \pi y_0}{b}\right)}{[(f_n^*)^2 - f^2]} \quad (5)$$

To derive expressions for M_2 , M_3 and M_{21} a plate with the configuration shown in figure (3(b)) is considered. In this case a moment is applied along on edge of the plate. The boundary condition are therefore simple supports along three edges, zero displacement and zero moment, and one edge pinned with an applied moment. Because of these uncommon boundary conditions the first task is to derive an expression for the mode functions and then use a series solution to derive the mobility functions. The displacement $u(x, y)$ can be given by an expression of the form [6,7]

$$u(x, y) = \sum_{n=1}^{\infty} \psi(y) \sin\left(\frac{n\pi x}{a}\right) \quad (6)$$

where $\psi(y)$ is a function of the boundary conditions in the y -axis direction. This function must satisfy the conditions

$$u(x, 0) = 0, \quad \frac{\partial^2 u(x, 0)}{\partial y^2} = 0$$

and

$$u(x, b) = 0, \quad \frac{\partial^2 u(x, b)}{\partial y^2} = \frac{-T(\chi)}{D^*} \quad (7)$$

where $T(\chi)$ is the applied moment along the plate edge. Using these boundary conditions and the general solution for the response in one direction, one can derive an expression for $\psi(y)$ to give, (the derivation of the following equations can be found in Appendix A)

$$u(x, y) = \sum_{n=1}^{\infty} \frac{T_n}{2\pi f a \sqrt{\rho h D^*}} \left[\frac{\sin(k_2 y)}{\sin(k_2 b)} - \frac{\sinh(k_1 y)}{\sinh(k_1 b)_1} \right] \sin\left(\frac{n\pi x}{a}\right) \quad (8)$$

where

$$T_n = \int_0^a T(\chi) \sin\left(\frac{n\pi x}{a}\right) dx \quad (9)$$

and the wavenumbers k_1 and k_2 are defined by [6,7]

$$\begin{aligned} k_1^2 &= 2k_x^2 + k_y^2 \\ k_2^2 &= k_y^2 \end{aligned} \quad (10)$$

where k_x and k_y are the plate flexural wavenumbers in the x and y directions respectively. Thus k_x and k_y satisfy the relationships

$$f^2 = \frac{D^*}{2\pi \rho h} (k_x^2 + k_y^2)^2$$

and

$$k_x = (n_1 \pi / a) \quad (11)$$

All wavenumber components are complex quantities to include the structural damping.

Equation (8) can be used to obtain M_2 , M_3 and M_{21} . However, before any of these mobility functions can be evaluated, an expression for T_n is required, which would require knowledge of the distribution of the moment along the plate's edge.

The distribution of this moment is a function of the type and location of the loading of the global structure. One way around this moment distribution dependency is to derive an overall function for $M_{12}/(M_2 + M_3)$ to be used in the power flow expression, equation (1) and then a separate expression for M_{21} . Also, each of these functions would be derived for each mode separately and the overall result obtained by summing all the contributions from all the modes. Thus after some manipulations starting from equation (8) the following relationships can be derived.

$$\left[\frac{M_{12}}{M_2 + M_3} \right]_{n_1} = \frac{\frac{2f(-1)^{n_2} n_2 \sin^2\left(\frac{n_1 \pi x_o}{a}\right) \sin\left(\frac{n_2 \pi y_o}{b_1}\right)}{\rho_1 h_1 a b_1^2 \left[(f_n^*)^2 - f^2 \right]}}{\sin\left(\frac{n_1 \pi x_o}{a}\right) [A + B]} \quad (12)$$

where

$$A = \frac{k_1 \coth(k_1 b_1) - k_2 \cot(k_2 b_1)}{a \sqrt{\rho_1 h_1 D_1^*}}$$

and

$$B = \frac{k_1 \coth(k_1 b_2) - k_2 \cot(k_2 b_2)}{a \sqrt{\rho_2 h_2 D_2^*}}$$

where the k_1 and k_2 in the equation for A for the source substructure, are different from those in the equation for B which is for the receiver substructure, and

$$\left[M_{21} \right]_{n_1} = \frac{-j}{a \sqrt{\rho h D^*}} \left[\frac{\sin(k_2 y_o)}{\sin(k_2 b_1)} - \frac{\sinh(k_1 y_o)}{\sinh(k_1 b_1)} \right] \sin\left(\frac{n_1 \pi x_o}{a}\right) \quad (13)$$

and for the particular case of two identical plates the overall power input obtained by substituting equations (3), (12) and (13) into equation (1) is given by

$$\frac{P_{in}}{|F(f)|^2} = \frac{2f}{\pi \rho_1 h_1 a b_1} \operatorname{Im} \left[\sum_{n=1}^{\infty} \frac{\sin^2 \left(\frac{n_1 \pi x_o}{a_1} \right) \sin \left(\frac{n_2 \pi y_o}{b_1} \right)}{[(f_n^*)^2 - f^2]} \right. \\ \left. \left\{ \sin \left(\frac{n_2 \pi y_o}{b_1} \right) - \frac{(-1)^{n_2} n_2 \pi}{2b_1} \right. \right. \\ \left. \left. \left[\frac{\sinh(k_1 y_o) \sin(k_2 b_2) - \sin(k_2 y_o) \sinh(k_1 b_1)}{k_1 \cosh(k_1 b_1) \sin(k_2 b_2) - k_2 \cos(k_2 b_1) \sinh(k_1 b_1)} \right] \right\} \right] \quad (14)$$

To obtain an expression for the transmitted vibrational power it is more important that the distribution of the moment along the joint edge is known. The transmitted power is given by the integral of the transmitted power per unit length over the entire length of the joint. For the special case of two identical plate substructures of equal size the expression for the transmitted power is given by

$$\frac{P_{trans}}{|F(f)|^2} = \left(\frac{2f}{\rho h a b^2} \right)^2 \\ \left[\sum_{n=1}^{\infty} \frac{\sin^2 \left(\frac{n_1 \pi x_o}{a} \right) \sin^2 \left(\frac{n_2 \pi y_o}{b} \right)}{[(f_n^*)^2 - f^2]^2} \frac{\operatorname{Real}\{[M_3]_{n_1}\}}{4 |[M_3]_{n_1}|^2} \right] \quad (15)$$

where

$$\begin{bmatrix} M_3 \end{bmatrix}_{n_1} = \frac{-j}{a\sqrt{\rho h D^*}} \begin{bmatrix} k_1 \coth(k_1 b) - k_2 \cot(k_2 b) \end{bmatrix}$$

Both expressions for the input and the transferred power are functions of the input loading position (x_0, y_0) and the material characteristics of the plates given by the density, thickness, area and natural frequencies.

Results

The input and transmitted vibrational power for an L-shape plate structure were computed using the above derived equations. However, it is necessary to verify the results and thus comparison is made with results obtained using FEA and SEA. Before proceeding to discuss the results a brief description of the FEA model is given. The package used for the FEA is the MARC finite element package [8].

The model for the L-plate consists of 63 nodes and 48 flat thin plate elements (element type 50 in MARC). The decision on the number of nodes was made after computing the required number of nodes required to achieve good accuracy in estimating the mean square velocity over the entire surface of the structure, up to a maximum frequency of 1 KHz. The total number of nodes was however slightly decreased to reduce the computation time. With 63 nodes good accuracy is expected up to 600 HZ. In fact this is the role to be played by FEA as a verification of the results at low frequencies. The FEA model of the plate is shown in figure (4). This is the model used for the modal analysis which had two extra rows of elements to obtain a better indication of the behavior (rotation) of the joint. During modal analysis the computation time is rather short and thus the addition of the extra two rows of elements were not a problem with computer run time.

FEA were used to compute both the natural frequencies and mode shapes and the response of the receiver plate when a harmonic force is applied to the source plate. Since this analysis was intended to be a verification of the power flow results, the same plate structural characteristics and point of excitation were used. The modal analysis was performed to ensure good correlation between the FEA model and power flow model.

In the harmonic analysis the model with 63 nodes was used. The objective of this multi-increment frequency analysis was to compute surface deflection data from which the spatial average velocity squared is obtained. The power transferred to the receiver plate, which is equal to the dissipated power by conservation of power, is given by

$$P_{trans} = \eta 2\pi f p a b h \langle |V_2(f)|^2 \rangle \quad (16)$$

where η is the receiver plate loss factor and $\langle \rangle$ denotes spatial averaging. In the spatial averaging of the velocity squared of the receiver plate, only the internal nodes were considered.

A number of excitation location were considered and two typical results for the transmitted power per unit force squared are shown in figures (5(a) and (b)). On the same figures are shown the power flow results and the results using the FEA. The frequency resolution used for the FEA is different for figures (5(a)) and (5(b)). For figure (5(a)) a resolution of 1 Hz was used in the frequency range between 1Hz and 100Hz and 10Hz resolution for the frequency range 110 to 1000Hz. In figure (5(b)) the frequency resolution is constant at 5Hz.

The results obtained using the power flow method for the transferred power were also compared to results obtained using SEA. With SEA a ratio of the transferred power to input power is usually given thus a ratio between the transferred and input power is obtained by dividing equation (15) by equation (14). Two sets of results for excitation in the middle of the source plate are shown in figure (6). The power ratio curve computed using the power flow technique show some anomalies, in that the ratio exceeds unity. These are due to resolution errors and infact occur close to the resonant peaks, where the exact definition of the peak is important. Also the computational method is breaking down at two frequencies, just above 400Hz and 800Hz. Both of these errors are currently being investigated.

As can be observed in figures (5) and (6) , good agreement is obtained between both the power flow and the SEA and FEA results. However, the computation for power flow is much more efficient compared to FEA when the spectrum of the transmitted power is required. Compared to SEA power flow is computationally more intensive, but the results obtained are closer to the actual response of the structure especially at the resonant frequencies.

Conclusion

In conclusion, a power flow technique has been presented in this paper which allows the computation of the response of a complex structure. What has been shown in this paper is the extension of the power flow technique to two-dimensional structures, and the results obtained match very closely with results obtained using FEA, but with potential saving in computation time. Also, the results are compared to results obtained using SEA and while the latter only predicts mean values for the response, the power flow method gives a better representation of the actual response of the structure.

In this paper, only the formulation of the power flow method for two-dimensional structures have been presented. However, having shown that the power flow method is a very powerful technique, and that it is not limited to one dimensional or solely point connected structures but can be

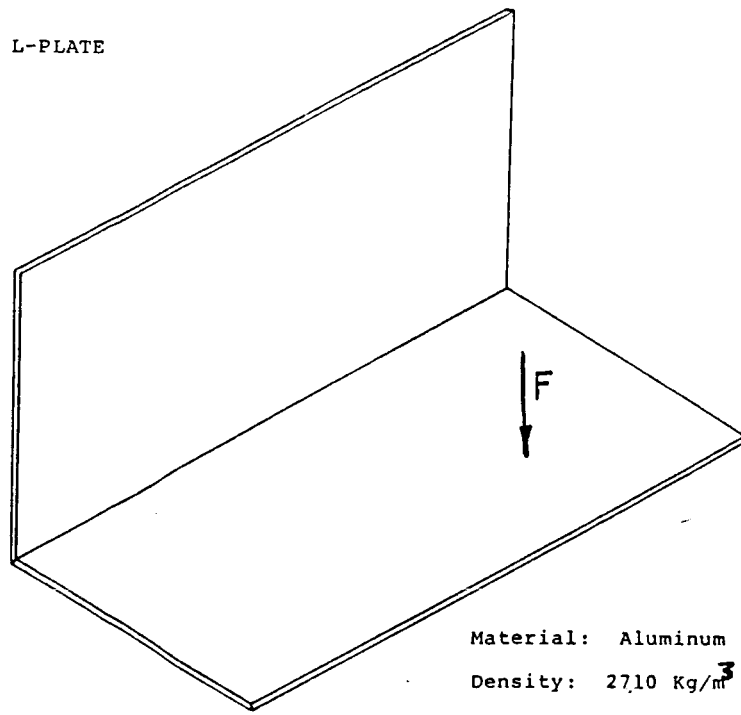
used for the analysis of two-dimensional structure, the influence of parameters of the structures and the excitation on the response of individual substructures will be investigated. Because of the fact that the power flow results represent the narrow band spectrum for the response, the effect of the structure and excitation parameters on the exact response of the structure can be deduced.

Additionally, the technique needs to be extended to more complex structures. This would require that the respective mobility functions used in the analysis be better defined than they are here. The shape of the moment function at the joint needs to be fully defined from which mobility functions for various condition can be derived and stored in a data base for future use. The analysis of a complex structure would then be an exercise in putting together the right mobility functions which would be available in the data base. The choice of the mobilities can be verified by comparing the very low frequency results and modal frequencies to results obtained using FEA, thus verifying the power flow model and the mobility functions used.

References

1. CUSCHIERI, J.M. "Power Flow as a Complement to Statistical Energy Analysis and Finite Element Analysis" to be published in the ASME Winter Annual Meeting 1987 Conference Proceedings, 1987.
2. PINNINGTON, R.J., WHITE, R.G. "Power Flow through Machine Isolators to Resonant and Non-Resonant Beams", Journal of Sound and Vibration 75, 179-197, 1981.
3. PINNINGTON, R.J. "Vibrational Power Transmission from Machines" Noise Con '87 Proceedings, 707-712, 1987.
4. CUSCHIERI, J.M., RICHARDS, E.J. "The Prediction of Total Loss Factors of Coupled Structures" Vibration Damping Workshop II "Damping '86" proceedings, GC-1, 1986.
5. CREMER, L., HECKL, M., UNGAR, E.E. "Structure-Borne Sound" Springer-Verlag, New York, 1973.
6. LEISSA, A.W. "Vibration of Plates", NASA SP 160, 1969.
7. BOISSON, C., GUYADER, J.L., MILLOT, P., LESUEUR, C. "Energy Transmission in Finite Coupled Plates, I and II. Journal of Sound and Vibration, 81 (1), 81-105, 1982.
8. MARC Analysis Research Corporation, "MARC General Purpose Finite Element Program", Palo Alto, California, 1986.

L-PLATE



Material: Aluminum
 Density: 2710 Kg/m^3
 Elastic Modulus: $7.2 \times 10^{10} \text{ N/m}^2$
 Thickness: 0.00635 m
 Dimensions: $1.0 \text{ m} \times 0.5 \text{ m}$
 Loss Factor: 0.01

Figure 1. Plate structure showing plate characteristics.

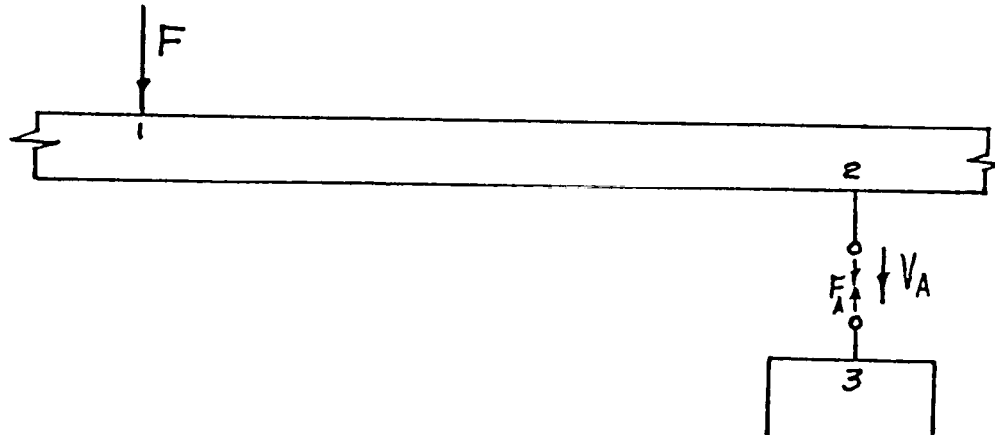


Figure 2. General power flow model.

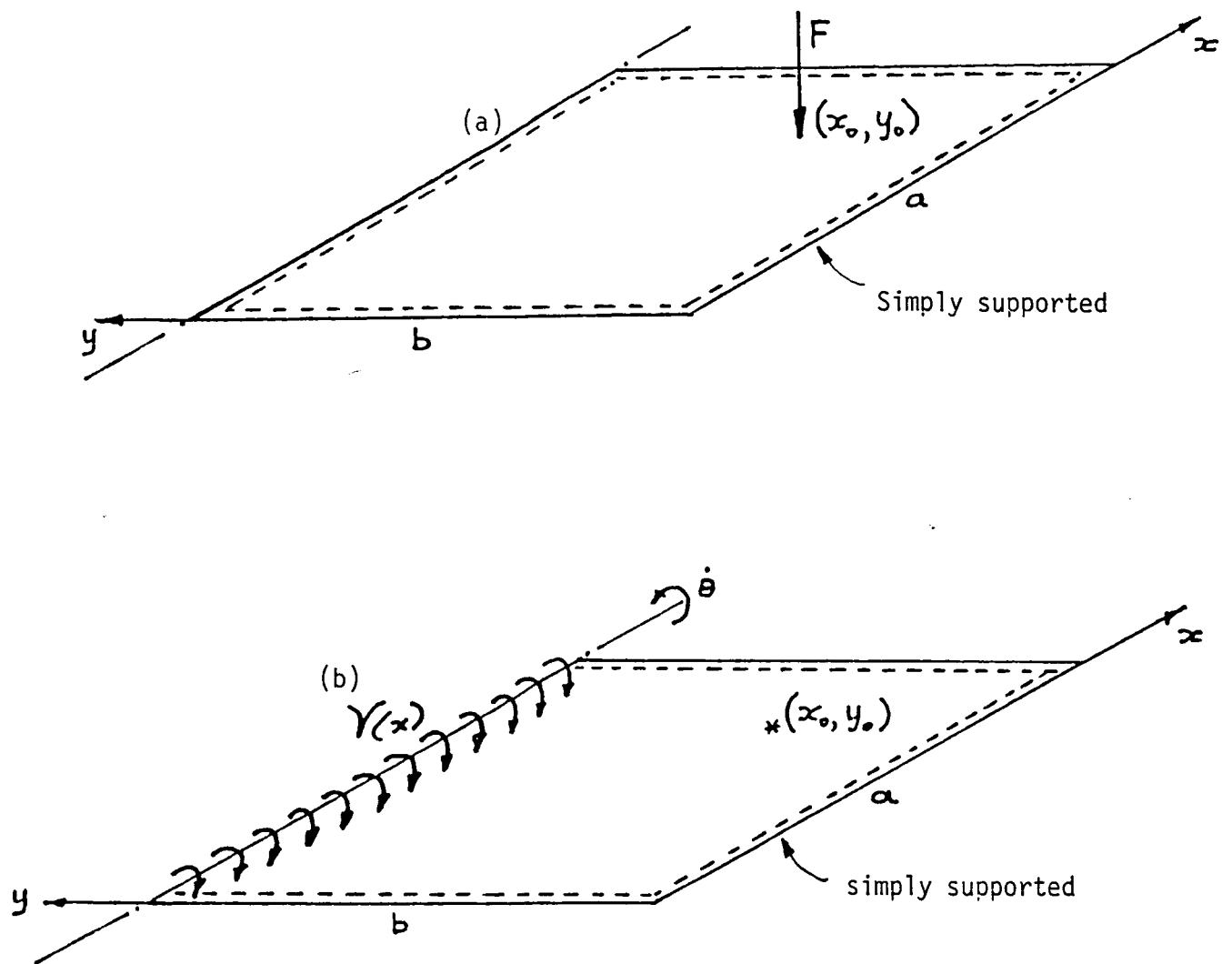


Figure 3. Power flow model substructural components of the L-shaped plate. (a) Plate with point excitation; (b) Plate with distributed edge moment excitation.

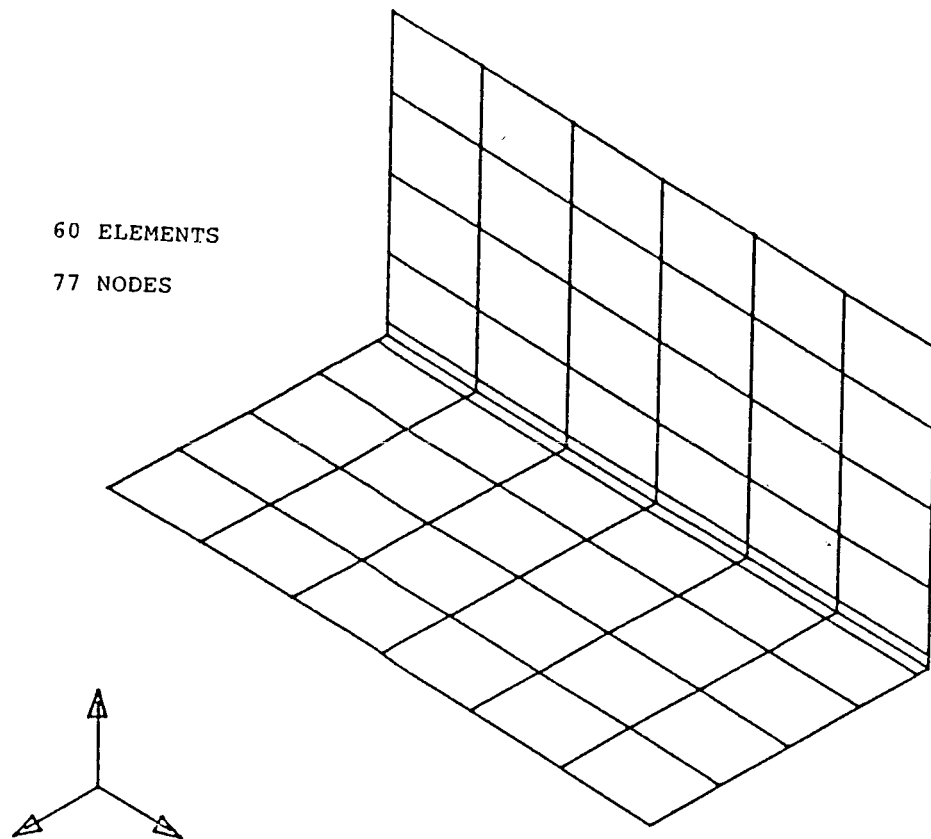


Figure 4. FEA model.

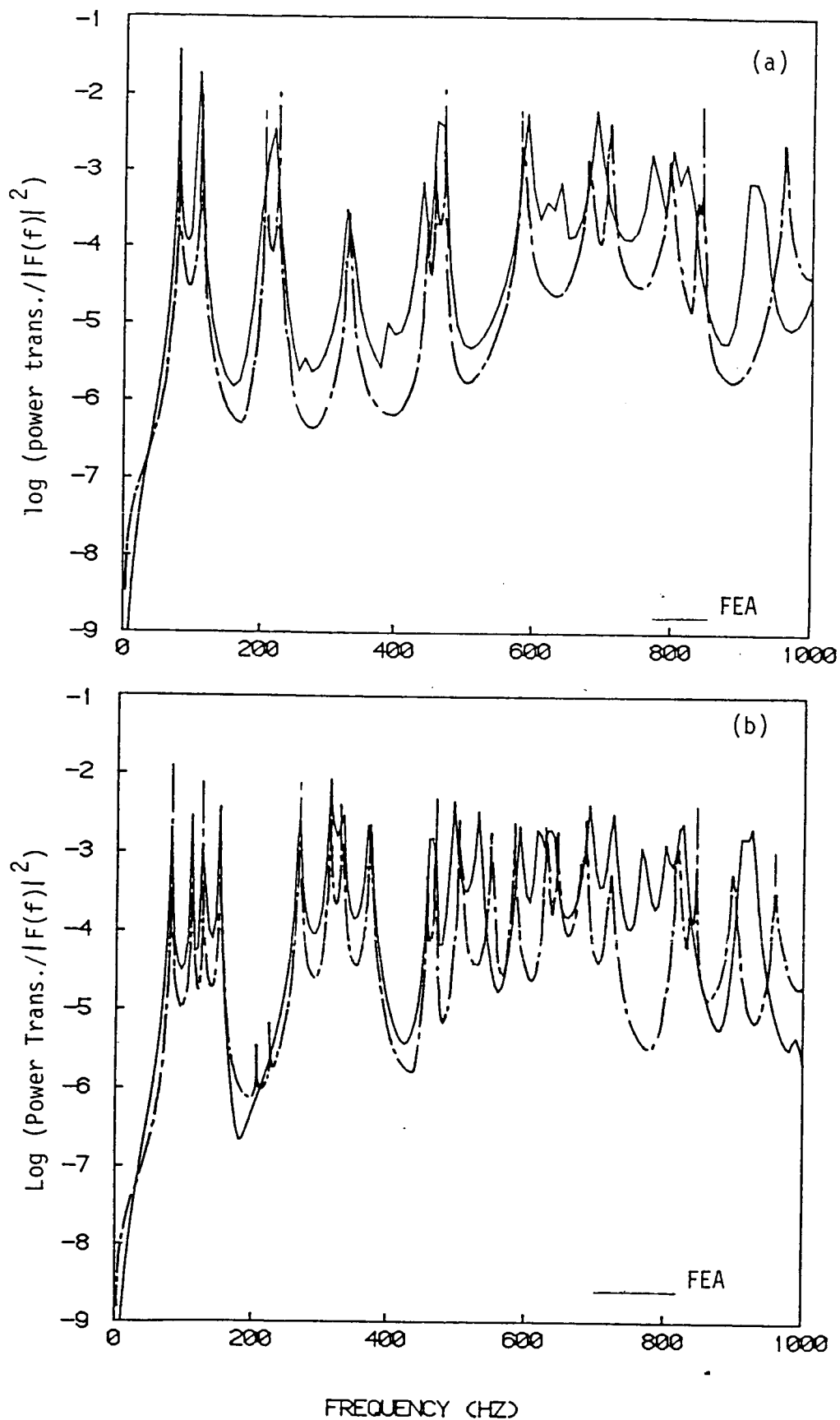


Figure 5. Results of the power flow analysis and the FEA for the transferred power. (a) Excitation in the center of the source plate; (b) Excitation off center.

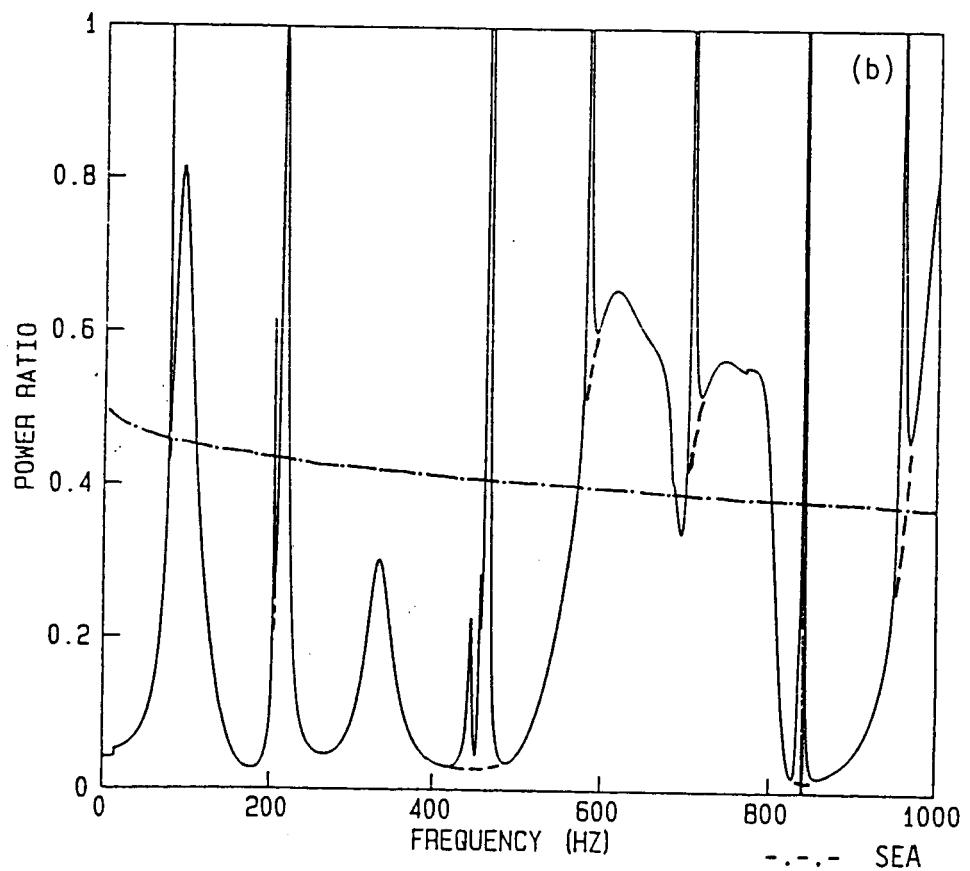
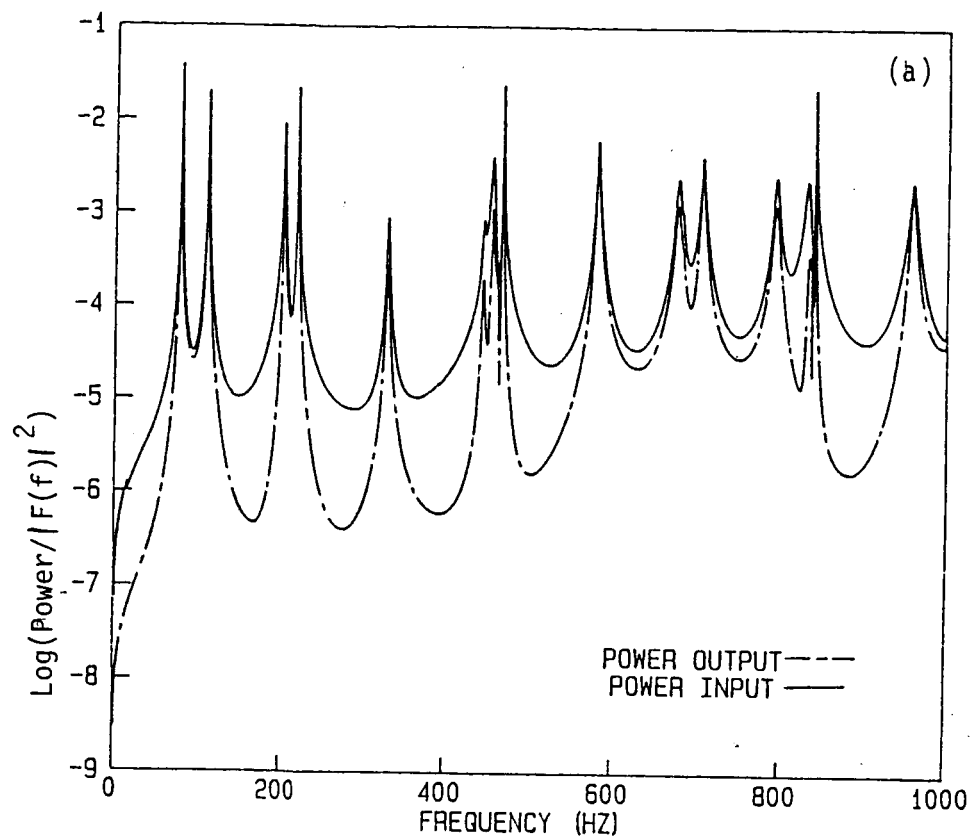


Figure 6. Ratio of power transmitted to power input and comparison with SEA results for excitation in the center of the source plate. (a) Comparison of transferred and input power; (b) power ratio and SEA results.

Appendix A

The mobility functions for the case of a plate simply supported along three edges, and pinned with a distributed moment applied along the fourth edge are derived as follows.

The displacement normal to the surface of the plate is given by equation (6) which satisfies the boundary conditions (see figure 3(b)),

$$\begin{aligned} u(0,y) &= 0, & u(a,y) &= 0 \\ \frac{\partial^2 u(0,y)}{\partial x^2} &= 0, & \frac{\partial^2 u(a,y)}{\partial x^2} &= 0 \end{aligned} \quad (A.1)$$

The function $\psi(y)$ in equation (6) is chosen such that the conditions given by equation (7) are satisfied. The expression for $\psi(y)$ is obtained by solving the one-dimensional differential equation $(\nabla^4 - k^4)u(x,y)=0$ in the y -axis direction. That is [7]

$$\psi(y) = A \cosh(k_1 y) + B \sinh(k_1 y) + C \cos(k_2 y) + D \sin(k_2 y) \quad (A.2)$$

where A, B, C, D are constants dependent on the boundary conditions in the y -axis directions, and k_1 and k_2 are defined in equations (10) and (11).

From the boundary conditions,

$$A = C = 0 \quad (A.3)$$

and to solve for B and D the distributed moment is spatial transformed into its wavenumber (or wavelength) components

$$T(x) = \sum_{n_1=1}^{\infty} T_{n_1} \sin \left[\frac{n_1 \pi x}{a} \right] \quad (A.4)$$

then

$$B = \frac{-T_{n_1}}{2\pi f a \sqrt{\rho h D^*} \sinh(k_1 b)} \quad (A.5)$$

and

$$D = \frac{T_{n_1}}{2\pi f a \sqrt{\rho h D} \sin(k_2 b)} \quad (A.6)$$

from which equation (8) is derived.

The distributed moment dependency from the mobility functions is eliminated by taking ratios of the mobilities. From the basic equation relating the motion of a coupled structure

$$\dot{\theta}_2(x, b) = \dot{\theta}_F(x, b) + M_2(x) T(x) \quad (A.7)$$

where $\dot{\theta}_2(x, b)$ is the angular velocity at the junction;
 $\dot{\theta}_F(x, b)$ is the angular velocity at the junction due to the application of the force F;
and $M_2(x) T(x)$ is the angular velocity due to the applied moment.

But the angular velocity at the junction must be the same for both substructural components,

$$\dot{\theta}_2(x) = \dot{\theta}_3(x) = -M_3(x) T(x) \quad (A.8)$$

and thus

$$\dot{\theta}_F = -(M_2 + M_3) T(x) \quad (A.9)$$

where the x dependency of M_2 and M_3 is suppressed for brevity. For M_2 and M_3

$$M_2 = \frac{\sum_{n_1=1}^{\infty} \left[\frac{\partial \psi_1(b_1)}{\partial y_1} \right] \sin\left(\frac{n_1 \pi x}{a}\right)}{\sum_{n_1=1}^{\infty} T_{n_1} \sin\left(\frac{n_1 \pi x}{a}\right)} \quad (A.10 \text{ a,b})$$

and similarly for M_3 , where for M_2 $i=1$ and for M_3 $i=2$. Along the x-axis direction both substructures have the same mode number. Thus

$$(M_2 + M_3) T(x) = \sum_{n_1=1}^{\infty} \left\{ \frac{\partial \psi_1(b_1)}{\partial y_1} + \frac{\partial \psi_2(b_2)}{\partial y_2} \right\}_{n_1} \sin\left(\frac{n_1 \pi x}{a}\right) \quad (A.11)$$

and from equation (A.9)

$$-\frac{[\dot{\theta}_F(x_o)]_{n_1}}{[T(x_o)]_{n_1}} = \left\{ \frac{\partial \xi_1(b_1)}{\partial y_1} + \frac{\partial \xi_2(b_2)}{\partial y_2} \right\}_{n_1} \sin\left(\frac{n_1 \pi x}{a}\right) \quad (\text{A.12})$$

where

$$[\xi_i(y_i)]_{n_1} = \frac{[\psi_i(y_i)]_{n_1}}{T_{n_1}} = \frac{1}{2\pi a f \sqrt{\rho h D^*}} \left[\frac{\sin(k_2 y_i)}{\sin(k_2 b_i)} - \frac{\sinh(k_1 y_i)}{\sinh(k_1 b_i)} \right] \quad (\text{A.13})$$

The advantage of $\xi(y)$ over $\psi(y)$ is that $\xi(y)$ is independent of the distributed moment. From equation (A.12)

$$\frac{[T(x_o)]_{n_1}}{F(f)} = \left[\frac{M_{12}}{M_2 + M_3} \right]_{n_1} = \frac{-[\dot{\theta}_F(x_o)]_{n_1} / (F(f))}{\left\{ \frac{\partial \xi_1(b_1)}{\partial y_1} + \frac{\partial \xi_2(b_2)}{\partial y_2} \right\}_{n_1} \sin\left(\frac{n_1 \pi x_o}{a}\right)} \quad (\text{A.14})$$

Substituting in equation (A.14) for the numerator by equation (5) and for the denominator by equation (A.13), equation (12) is obtained.

From definition

$$M_{21}(x) = V_F / [T(x)] \quad (\text{A.15})$$

where V_F is the velocity at the excitation point due to the moment applied along the edge. Thus from equation (8)

$$[M_{21}]_{n_1} = \frac{j}{a \sqrt{\rho h D^*}} \left[\frac{\sin(k_2 y_o)}{\sin(k_2 b_1)} - \frac{\sinh(k_1 y_o)}{\sinh(k_1 b_1)} \right] \sin\left(\frac{n_1 \pi x_o}{a}\right) \quad (\text{A.16})$$

By combining equations (A.14) and (A.16) the expression for the input power (equation 14) is obtained.

The transmitted power to the receiver substructure is given by the integral over the entire length of the joint:

$$P_{\text{trans}} = \frac{1}{2} \int_0^a \text{Real} \left\{ T(x) \dot{\theta}_3^*(x) \right\} dx \quad (\text{A.17})$$

For the case of two identical plate substructures, using the basic relationship

$$\dot{\theta}_3(x) = \frac{-M_3}{M_2 + M_3} \dot{\theta}_F = \frac{-\dot{\theta}_F}{2} \quad (\text{A.18})$$

$$P_{\text{trans}} = \frac{1}{2} \text{Real} \int_0^a \left\{ \left[\sum_{n_1=1}^{\infty} \frac{\left[\frac{-\dot{\theta}_F(x)}{2} \right]_{n_1}}{2 \left[\frac{\partial \xi_1(b_1)}{\partial y_1} \right]_{n_1}} \right] \left[\sum_{n_1=1}^{\infty} \frac{\left[\frac{-\dot{\theta}_F(x)}{2} \right]_{n_1}^*}{2} \right] \right\} dx \quad (\text{A.19})$$

Both terms within the integral are sinusoidal functions and represent different modes of the structure for different values of n_1 . Due to orthogonality of the modes equation (A.19) simplifies to:

$$\frac{P_{\text{trans}}}{|F(f)|^2} = \frac{1}{2} \sum_{n_1=1}^{\infty} \text{Real} \left\{ \frac{\left[\xi_{F_o_o}(x, y) \right]_{n_1}^2}{4 \left[\frac{\partial \xi_1(b_1)}{\partial y_1} \right]_{n_1}} \right\} \quad (\text{A.20})$$

where

$$\left[\xi_{F_o_o}(x, y) \right]_{n_1} = \frac{\left[\dot{\theta}_{F_o}(x) \right]_{n_1} / [F(f)]}{\sin \left[\frac{n_1 \pi x_o}{a} \right]} \quad (\text{A.21})$$

Substituting in equation (A.20) by equations (A.13) and (8), the expression for the transmitted power, equation (15) is obtained.

Appendix B

Experimental Analysis Of Power Transmission In An L-shaped Beam

Introduction

An experimental analysis was performed on an L-shaped beam structure (figure B.1). The objective of the experiment was to measure the power transmitted from the source beam to the receiver beam, which was excited by a harmonic force at one end. The results are compared to those obtained in the analytical study [1]. The experimental procedure is to measure the response at several points on the receiver beam and to obtain a spatial average of the square of the normal surface velocity over these points. In using this method, it is assumed that the power transmitted to the receiver beam is equal to the power dissipated since the beam is not connected to anything other than the source beam. The time averaged power dissipation in a finite structure is given by equation (16).

Experimental Setup

The experimental setup consists of two identical steel beams of thickness $3/8$ inch (0.0095m), width 3 inches (0.0762m), and length 36 inches (0.9144m). The beams are welded to a $5/8$ inch (0.0159m) diameter steel rod such that these form a 90 degree angle at the joint (figure B.1). The rod provides a means of pinning the joint so that the experimental setup matches the boundary conditions used in the theoretical analysis. The rod was held by two flange bearings mounted to a base structure. The harmonic excitation is provided by means of a Wilcoxon electromagnetic shaker attached to the source beam via an impedance head and supported by a heavily damped support rig.

The experiment consists of two parts:

- 1) Determination of the damping loss factor
- 2) Measurement of the spatial average velocity of the beams and the processing to obtain the dissipated power.

The structural damping was measured using both the decay method and the half-power bandwidth method. The measurements were performed using a calibrated impact hammer, with an accelerometer at the end of the second beam. This measurement point was chosen because it does not represent a node at any of the natural frequencies. From damping measurements on the undamped L-beam it was determined that the bearings and the exciter attachment to the beams were the main source of energy dissipation. Since this would create undesirable effects in doing the measurements, viscoelastic material was added to one side of each beam.

Damping measurements were again performed for the damped L-beam when freely suspended and when mounted in its support rig and the shaker attached. For the latter case the damping was measured using a single frequency excitation and measuring the decay after the excitation is

switched off. The results of the damping measurements are shown in Table (B.I). It was observed that the addition of the viscoelastic material increased the damping sufficiently such that the influence of the bearings had little effect on the structural damping.

In the second part of the experiment, the transverse acceleration response due to band limited white noise excitation was measured at ten uniformly spaced points on the receiver beam. The acceleration measurements were made using a B&K 4375 accelerometer. The data was processed according to the following procedure.

- 1) A transfer function was first obtained between the spectra of the acceleration response data and the force data using an HP 5451C structural dynamics analyzer.

- 2) The frequency domain data were then divided by $j2\pi f$ to obtain the velocity response and then squared.

- 3) These two steps were performed at each of the ten measurement points with the resulting ten sets of data averaged to obtain the spatial averaged velocity squared per unit input force squared. The frequency range used was between 0 and 1.25 KHz.

- 4) Finally the data was multiplied by the measured damping loss factor and the beam mass and frequency to obtain the dissipated power.

Results

The measurement results for the power transmitted to the receiver beam are compared with the results given by the power flow method in figure (B.2). There are several comments which can be made about these results. First there is good agreement between the measured data and the analytical predictions in terms of the natural frequencies of the coupled system. In general any offset of peaks in the measurement curve from the peaks in the power flow curve may be attributed to insufficient frequency resolution in the measurements. Some discrepancies in level are obtained at the resonant frequencies which also may be due to resolution. Below 100 Hz it is difficult to draw any conclusions about the measured data. The cutoff frequency of the electrodynamic shaker and power amplifier is 20 Hz which makes the data below this frequency unreliable. The discrepancies in the results in the 40 to 100 Hz range are attributed to vibration of the supporting structure, both for the beam and the electrodynamic shaker. Additionally there are two peaks (at 112 Hz and 218 Hz) in the measured data which do not appear in the analytical results. These are attributed to support structure resonances. However in general there is reasonable agreement between the analytical and the experimental results.

Work is still in progress to measure the power flow vectors along the two beam substructures. Two techniques are being used which differ in the number of accelerometers used in the measurements. Some results have been obtained with a two accelerometer arrangement [B.1], however the results

obtained thus far have not been fully explained. A possible reason for the unexpected results is the very large standing wave ratio which is the ratio of the amplitude of the standing wave to the propagating wave. This may possibly not allow us to do these type of power flow measurements using this arrangement. An alternative is to use a three accelerometer configuration [B.2] however no results have yet been obtained using this technique.

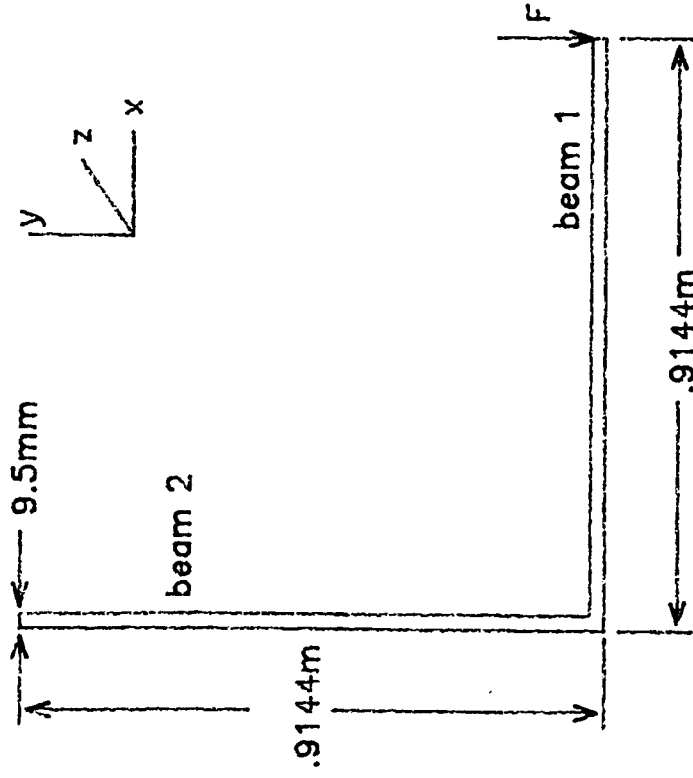
References

B.1 Redman White W. "The Measurement of Structural Wave Intensity", Ph.D. Thesis, Southampton University, Southampton England, 1983.

B.2 Bouyaakoub N. "Mesure Du Flux D'energie Vibratoire Dans Les Structures", Joint Report Universite De Technologie De Compiene/ EDF Clamart Der, France, 1986, (In French).

TABLE B.I

Mode #	<u>Measured Damping Loss Factors</u>			
	Free Undamped	Free Damped	Pinned Damped	Pinned, damped (shaker Attached)
1	0.005	0.011	0.007	
2	0.004	0.012	0.008	0.008
3	0.003	0.008	0.006	0.010
4		0.008	0.009	0.018
5		0.008	0.008	0.020
8		0.009	0.012	0.017
9		0.009	0.012	0.018



Material: Steel
 Density: 8000 Kg/m^3
 Modulus of
 Elasticity: 200 GN/m^2
 Loss Factor: 0.01

Figure B.1. L-shaped beam structure.

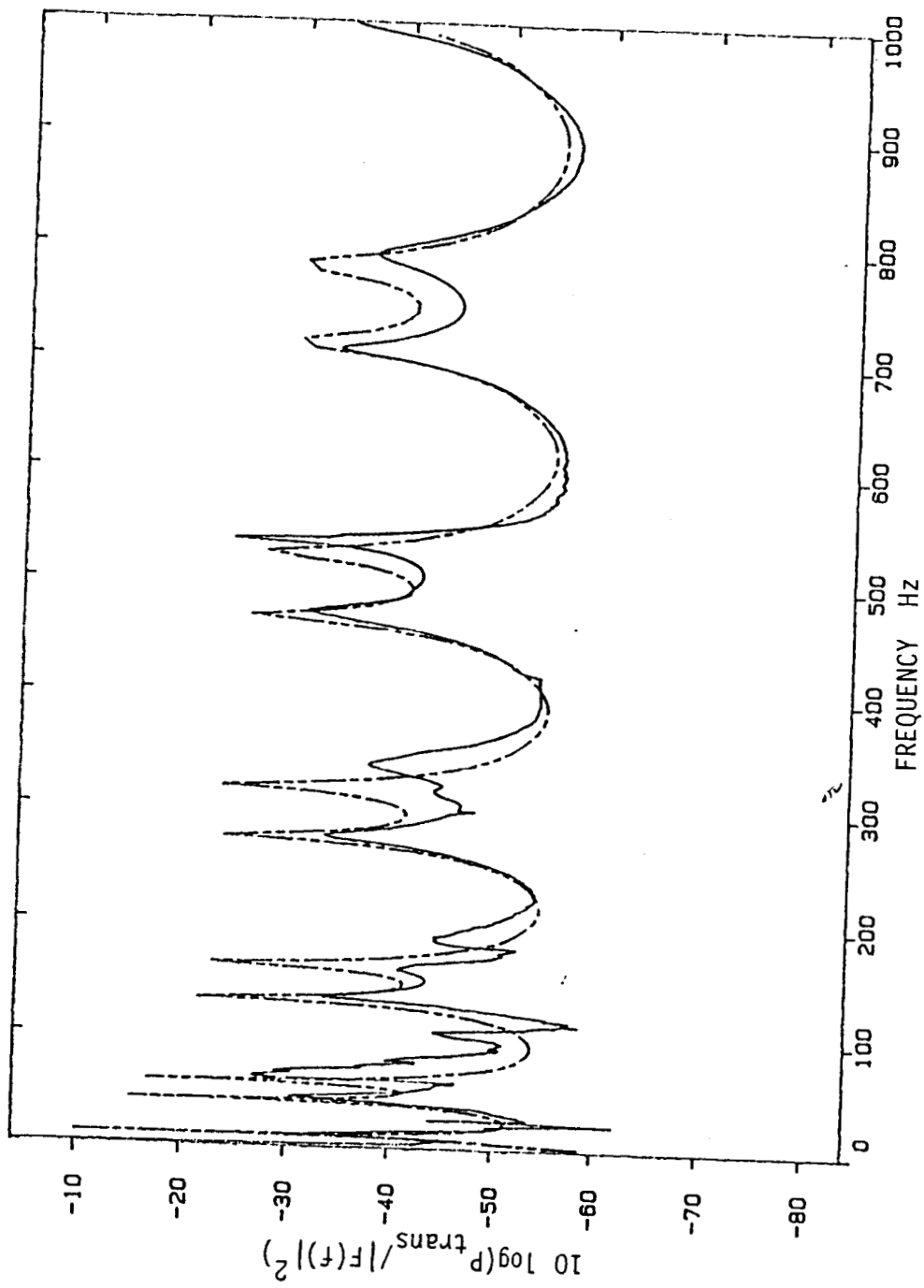


Figure B.2 Measured power transferred per unit input force squared for the L-shaped beam structure. —: experimental results; -.-: analytical results.